Environmental Science & Technology

Article

pubs.acs.org/est

Fast Deswelling of Nanocomposite Polymer Hydrogels via Magnetic Field-Induced Heating for Emerging FO Desalination

Amir Razmjou,[†] Mohammad Reza Barati,[‡] George P. Simon,*[,‡] Kiyonori Suzuki,[‡] and Huanting Wang*[,†]

[†]Department of Chemical Engineering, [‡]Department of Materials Engineering, Monash University, Clayton, Victoria 3800, Australia

Supporting Information

ABSTRACT: Freshwater shortage is one of the most pressing global issues. Forward osmosis (FO) desalination technology is emerging for freshwater production from saline water, which is potentially more energy-efficient than the current reverse osmosis process. However, the lack of a suitable draw solute is the major hurdle for commercial implementation of the FO desalination technology. We have previously reported that thermoresponsive hydrogels can be used as the draw agent for a FO process, and this new hydrogel-driven FO process holds promise for further development for practical application. In the present work, magnetic field-induced heating is explored for the purpose of developing a more effective way to recover water from swollen hydrogel draw agents. The composite hydrogel particles are prepared by copolymerization of sodium acrylate and *N*-isopropylacrylamide in the presence of magnetic nanoparticles (γ-Fe_2O_3, <50 nm). The results indicate that the magnetic heating is an effective and rapid method for dewatering of hydrogels by generating the heat more uniformly throughout the draw agent particles, and thus, a dense skin layer commonly formed via conventional heating from the outside of the particle is minimized. The FO dewatering performance is affected by the loading of magnetic nanoparticles and magnetic field intensity. Significantly enhanced liquid water recovery (53%) is achieved under magnetic heating, as opposed to only around 7% liquid water recovery obtained via convection heating. Our study shows that the magnetic heating is an attractive alternative stimulus for the extraction of highly desirable liquid water from the draw agent in the polymer hydrogel-driven forward osmosis process.

INTRODUCTION

Stimuli-responsive hydrogels are versatile materials able to contribute significantly to a number of areas, such as the biochemical and biomedical areas.[1] This broad range of applications is due to the variety of choice of environmental stimuli that can be used to tune their properties, such as changes in temperature, pH, electric fields, and ion strength.[2] Temperature is one of the most common stimuli, and one of the most used thermosensitive hydrogels is the poly(*N*-isopropylacrylamide) (PNIPAM)-based hydrogels due to their ability to undergo a phase transition in water at around 33 °C, known as the lower critical solution temperature (LCST). At or above LCST, the hydrophilic−hydrophobic balance of the hydrogel changes and causes the pendant hydrophobic isopropylamide groups to become dominant and induces deswelling and releasing of the entrapped water molecules and other water-soluble materials trapped in the hydrogel network.[3]

The main weakness of these temperature−stimuli-sensitive hydrogels is that their response and deswelling rate is too slow at or above the LSCT as a result of the case hardening phenomenon and the formation of a dense skin layer that limits the outward diffusion of water molecules, thereby slowing its water release rate.[4] The most convenient way to make the fast-acting hydrogels is to reduce the hydrogel dimensions, but small hydrogel particles are not suitable for many applications, such as artificial organs and actuators, because a certain dimension of hydrogel is required for these particular applications.[2] As a result, researchers have tried to improve the deswelling rate of such hydrogels fundamentally and practically by means of physical means (inducing porosity via freeze-drying,[5] phase separation,[6] and addition of pore-formers such as SiO_2[7] and PEG[8]) and chemical (introducing hydrophilic[9] or amphiphilic[10] moieties into hydrogel network) alterations of the hydrogels.

We have recently disclosed a new use for hydrogel particles as a new class of draw agent in the emerging forward osmosis (FO) desalination process, a technique seeking to address the global issue of freshwater scarcity.[11] In a typical FO desalination process, an osmotic pressure gradient is induced by a draw agent to provide the driving force for water molecules to pass through the membrane from the low osmotic pressure (saline water) to the high osmotic pressure (draw agent) side (see

Received: January 31, 2013
Revised: May 8, 2013
Accepted: May 13, 2013
Published: May 13, 2013

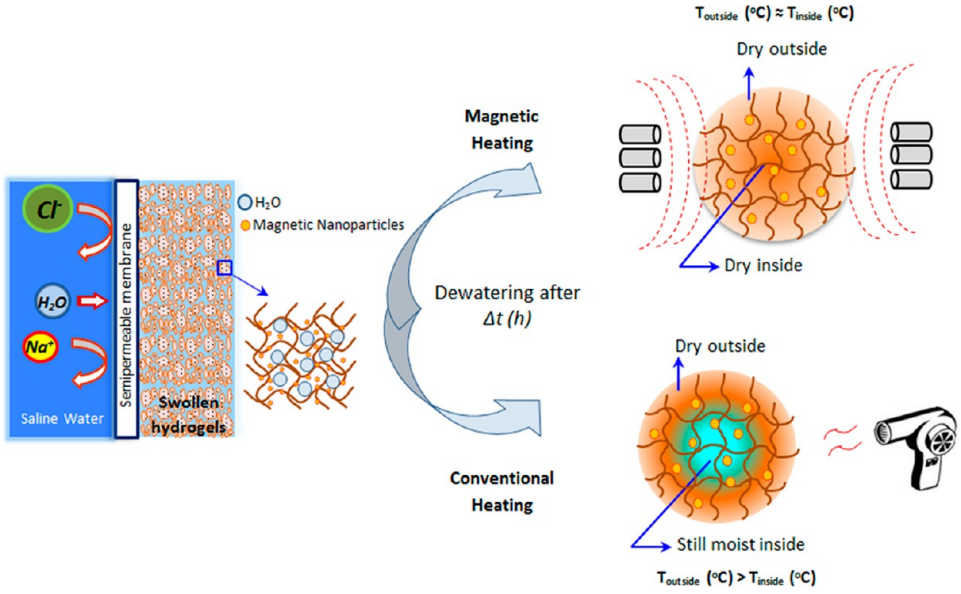

Figure 1. Schematic diagram of the effect of magnetic and conventional heating on the dewatering of nanocomposite polymer hydrogels being used as draw agents in the FO process.

Figure 1).[12] The water drawn through the membrane must then be readily able to be won back, with the whole process being continuous. To date, the most widely used chemicals have been ammonium bicarbonate, which can then be removed from the fresh water by thermal decomposition of the ammonium salt at about 60 °C. However, this process is found to be not suitable for producing high quality drinkable water, and we have found that appropriate hydrogel particles are able to perform this function of both attracting water via osmotic pressure and then being stimulated to release the water. Any new draw agent must meet the quality criteria, such as nontoxicity, particularly for potable water production; near neutral pH; compatibility with the membrane surface; and low-cost energy regeneration.[12] The polymeric hydrogel networks with three-dimensional interconnected structure and highly concentrated hydrophilic groups can relax and capture large volumes of water. The addition of ionic groups into the hydrogel network can further significantly increase the water uptake capacity and flux due to higher osmotic pressures. However, introducing the ionic groups into the hydrogel network compromises the thermoresponsive property and deswelling rate of hydrogels by enhancing the LSCT and, thus, the impact of case-hardening. In addition, higher LSCT and denser skin layers cause the water molecules to travel out of the hydrogel networks, mostly in the vapor, rather than the liquid phase. Therefore, the ability to rapidly recover a high yield of liquid water from the hydrogel particles is crucial for the viability of this new FO process.

Magnetic composite hydrogels have been studied for a wide variety of potential applications, such as controlled drug release,[13] hyperthermia treatments,[14,15] and chemomechanical devices.[16] Introducing the magnetic nanoparticles into hydrogels provides an effective way to remotely control and tune the nanocomposite. Surface-functionalized hydrophilic magnetic nanoparticles were recently reported as a draw solute and readily recovered by a uniform magnetic field.[17] The main drawback of this type of draw solute was the agglomeration of the nanoparticles after recovery, which led to decreased osmotic pressures and, thus, lowered flux.[18] Ling et al. have recently attempted to address the issue of agglomeration during the draw solute regeneration by preparing thermosensitive superparamagnetic nanoparticles.[19]

Here, we report our attempts to achieve fast deswelling of polymer hydrogel particles by incorporating magnetic nanoparticles, thus enabling magnetic heating as the temperature stimuli. Our results show that magnetic heating is a quicker and more effective way to extract the water from the hydrogel network. Unlike other conventional heating methods, the magnetic heating can result in a significantly lower temperature gradient, consequently retarding the effects of the case-hardening phenomenon. This technique leads to a high uniformity of warming throughout the whole volume of hydrogels, more precise temperature regulation, and a higher water recovery rate compared with conventional heating (see Figure 1). Another benefit is that the hydrogels can be heated in the membrane module, since the magnetic field is virtually unaffected by the external isolating layers and does not depend on the thermal conductivity. Likewise, heating is directed precisely to where it is required, rather than needlessly heating all components of the module.

In this work, the effect of incorporation of the magnetic nanoparticle (γ-F_2O_3, <50 nm) into the hydrogel network on the morphology and chemistry of the nanocomposite hydrogels was studied. The swelling behavior and kinetics, as well as water flux and deswelling performance of the new nanocomposite hydrogels, were investigated. On the basis of our previous works,[11,20] a copolymer of sodium acrylate and *N*-isopropylacrylamide with an equimolar ratio was selected in this study as an appropriate draw agent to be the nanocomposite matrix to demonstrate this new process.

EXPERIMENTAL SECTION

Materials. The sodium acrylate (SA, 99%) and *N*-isopropylacrylamide (NIPAM, 96%) monomers, ammonium persulfate (APS, ≥98.0%) initiator, *N*,*N*′-methylenebisacrylamide (MBA, 99%) cross-linker, iron(III) oxide nanoparticles (γ-F_2O_3) (particle size <50 nm, lot no. MKBD4890 V), dialysis bag (high retention seamless cellulose tubing, MW = 11 033)

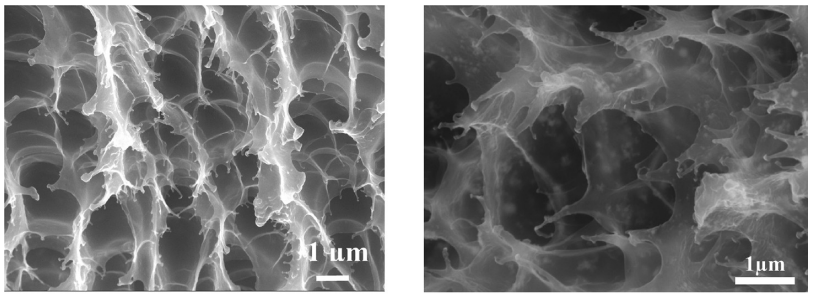

(a) (b)

Figure 2. SEM images of nanocomposite hydrogels with (a) 0 and (b) 16 wt % iron(III) oxide nanoparticles.

for swelling studies were all purchased from Sigma-Aldrich. Note that γ-F_2O_3 was selected because of its excellent chemical stability, although Fe_3O_4 has a slightly better magnetic property than γ-F_2O_3. Forward osmosis (FO) cartridge membranes made from cellulose triacetate with an embedded polyester screen mesh were provided by Hydration Technologies Inc. (Albany, OR).

Preparation of Nanocomposite Hydrogel Synthesis. Free-radical polymerization of monomers (NIPAM and SA) was the process to synthesize the magnetic nanocomposite hydrogels. First, an equimolar ratio (1:1) of SA and NIPAM monomers (2 g of SA and 2 g of NIPAM) were dissolved in 18.26 g of deionized water (DI) at room temperature in a capped bottle to form a 16.7 wt % solution. Afterward, 0.057 g of the MBA cross-linker was dissolved in the monomer solution.[11,20] Different concentrations of magnetic nanoparticles (MNPs) were then added to the solution with mild shaking (the weight percentage (wt %) of Fe_2O_3(g)/ (NIPAM + SA)(g) was set to 0, 2, 4, 8, and 16). A 0.04 g portion of ammonium persulfate was dissolved into the solution after the addition of the MNPs to initiate polymerization. The molar ratio of monomers, cross-linker, and initiator was fixed at 50:1:0.5. A probe sonicator (Misonic sonicators 3000) at amplitude of 20 and power of 18 W was used both to ensure good MNP dispersions in the polymer hydrogel and to raise the solution temperature. The sonication was continued until the temperature reached above 70 °C, at which point the solution suddenly turns into a gel, and the MNPs were fixed into the network without the chance for reagglomeration. The hydrogels were then kept at 70 °C overnight to ensure the termination of polymerization. To remove any unreacted reactant, the resultant hydrogels were immersed into deionized daily fresh water at room temperature for 3 days, followed by drying at 80 °C in a convection oven. Finally, the hydrogels were ground into fine particles (2−25 μm) cryogenically by utilizing a SPEX 6870 Freezer/Mill (SPEX SamplePrep.)

Characterization. The morphology of dry and swollen hydrogel particles was characterized by FESEM (JSM-7001F microscope, JEOL). Samples were sputter-coated with platinum to make them conductive. To observe the morphology of the swollen hydrogels, they were freeze-dried before sputter-coating. A Fourier transform infrared spectrometer (Perkin-Elmer Spectrum 100) was used to analyze the chemical structure of the nanocomposite hydrogels. A vibrating sample magnetometer (VSM) was employed to study the magnetic properties of nanocomposite hydrogels. Each sample for magnetic measurements weighed 5 mg; the total weight of the nanocomposite polymer hydrogel in a batch was 2 g. The nanocomposite hydrogels XRD patterns were recorded using a Philips PW 1140 diffractometer with nickel-filtered Cu Kα radiation (λ = 1.5406 Å). The step size and scanning rate were 0.01 and 0.1°/min, respectively. The swelling behavior, forward osmosis performance, and water recovery of nanocomposite hydrogels were all studied by utilizing the gravimetric methods and calculating the swelling ratio (Q), water flux (LMH), liquid water recovery (R_l), vapor water recovery (R_v), and total water recovery (R_t) (see the Supporting Information for more details).

RESULTS AND DISCUSSION

The existence and crystallinity of the nanocomposite hydrogels were investigated by XRD analysis for nanocomposite hydrogels with different concentrations of iron(III) oxide nanoparticles (see Figure S2 in the Supporting Information). The X-ray diffraction spectra of the pure hydrogel did not show any sharp or intense peaks, demonstrating the highly amorphous nature of the pure hydrogel formed from free radical polymerizations. Highly intense peaks did occur in the XRD pattern with an increase in the MNPs loading in the hydrogel matrix, which is consistent with the nanoparticles being incorporated. Fourier transform infrared spectrum (FT-IR) spectra of the nanocomposite hydrogels were used to study the chemical structure of the nanocomposite hydrogels (see Figure S3 in Supporting Information). From the FT-IR spectra, the so-called Fe−O range of iron(III) oxide (350−1000 cm^{-1})[1] becomes more distinct as the concentration of iron(III) oxide increases. A new strong peak at around 1066 cm^{-1} and a weaker one at around 1250 cm^{-1} could be attributed to the vibration of C−O bond on the γ-Fe_2O_3 magnetic nanoparticles after incorporating them into the hydrogel network.[2] These peaks at the higher MNP loading are likely due to the interaction between the MNPs and the hydrogel network via an interaction of Fe−O−C bonds in which the carboxyl groups could be associated with the surface of the γ-Fe_2O_3 magnetic nanoparticles through an intermediate oxygen.[3]

The quality of the dispersion of the MNPs within the hydrogel matrix and the morphologies of nanocomposite hydrogels with different concentrations of MNPs were studied by SEM and EDS mapping (see Figure S4 in the Supporting Information). As can be seen, the effect of the inclusion of MNPs on the general macrostructure of the nanocomposite hydrogels is not significant for dry, nonswollen hydrogels (bottom right inset images in Supporting Information Figure S4); they can appear as increased surface roughness of the 16 wt % MNPs-hydrogel samples. On the other hand, macrostructural changes were noticeably apparent after the nanocomposite hydrogels were swollen and freeze-dried. From the figure, increasing the concentration of MNPs reduced the cross-

linking density while increasing the network wall thickness. This reduction in the cross-linking density could be due to the presence of iron(III) oxide nanoparticles and its steric effect, which restricts the mobility of growing polymer chains and thus reducing the probability of the curing reaction.[21,22]

Although the primary particle size of iron(III) oxide nanoparticles is <50 nm (see the 100 wt % iron(III) oxide SEM image in Supporting Information Figure S4), their size in the polymer network increases at a higher MNPs content level and is indicative of their agglomeration, which could amplify the steric effect and, thus, lower the cross-linking density. The EDS mapping of the nanocomposite hydrogels (top right inset images in Supporting Information Figure S4) shows that the MNPs were mostly agglomerated on the hydrogel networks, particularly on the thick network walls. The morphology of nanocomposite hydrogels was also investigated at a higher magnification in Figure 2. Comparing the morphology of the hydrogels with the 16 wt % (Figure 2b) and 0 wt % (Figure 2a) MNP content revealed that the nanoparticles are dispersed throughout the matrix of hydrogels, and there is a good affinity between the organic and inorganic phases.

A vibrating sample magnetometer (VSM) was used to measure the magnetic properties of the nanocomposite hydrogels. The results in Figure 3a show the hysteresis curves and magnetic properties of nanocomposite hydrogels with different weight fractions of iron(III) oxide nanoparticles. The hysteresis loops of the nanocomposite hydrogels show remanent magnetization and coercivity at room temperature due to the ferrimagnetic behavior of dispersed nanoparticles with a mean particles size of <50 nm in the nanocomposite hydrogels. The saturation magnetization (σ_s) of the samples is between 1 and 62 (emu/g). The saturation magnetization (σ_s), remanent magnetization (σ_r), and coercivity (H_c) for bare γ-Fe_2O_3 are 62 (emu/g), 21.8 (emu/g), and 182.8 (Oe), respectively.

For the nanocomposites, there is a significant decrease in the magnetization. Such a large reduction of saturation magnetization could be related to the reduction in the concentration of the magnetic nanoparticles in the hydrogel network. It should be pointed out here that the slight changes in the coercivity values can be attributed to the degree of dispersion of the magnetic nanoparticles on the magnetostatic interaction among the magnetic particles.[23] The obtained VSM results in conjunction with XRD data indicate that no additional new magnetic phases or oxidized phases have been introduced into the nanocomposite hydrogel during the preparation process.

The degree of dispersion of nanoparticles into the hydrogel network has been characterized using quantitative analysis of varying weight fractions of magnetic nanoparticles by measuring the maximum magnetization (σ_s) of the samples at 5 kOe. According to our experimental design, the nominal weight fractions of the magnetic nanoparticles at the point of incorporation into the hydrogel network are 0, 2, 4, 8, and 16 wt %; however, the actual weight fraction may deviate from these nominal values because of poor dispersion, unreacted monomers, and precipitation of particles before the termination of polymerization. The real weight fraction is calculated from the equation

$$\text{actual weight fraction (wt \%)} = \sigma_{sn} \times \frac{100}{M\sigma_{s100}} \quad (1)$$

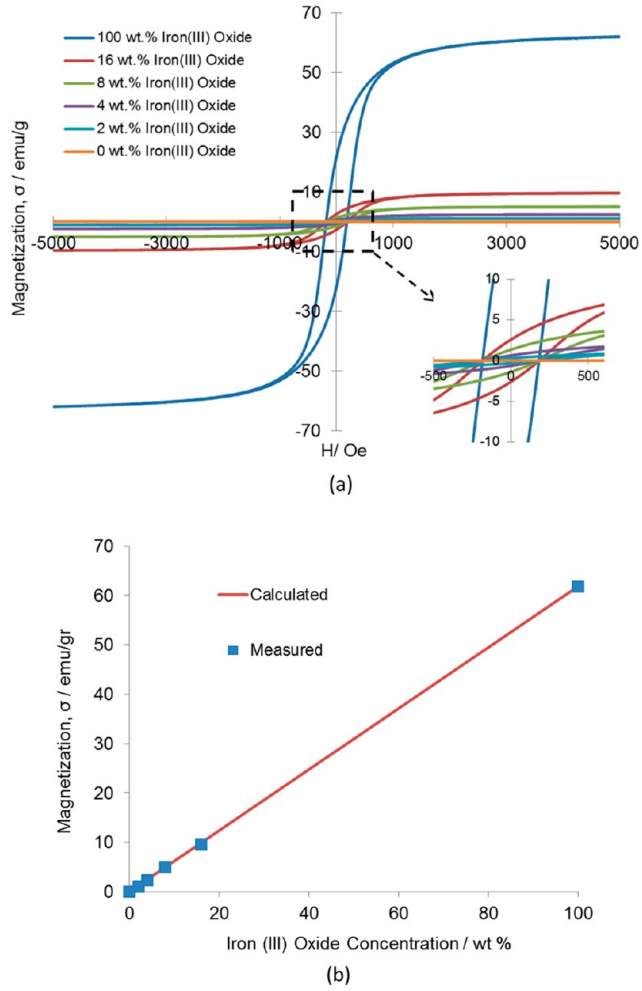

Figure 3. Magnetization curves of hydrogel nanocomposite prepared with (a) different weight fractions of MNPs at a maximum magnetic field of 5 kOe and (b) saturation magnetization versus the concentration of magnetic nanoparticles in the nanocomposite hydrogels.

where, σ_{sn} is the magnetization of each sample and σ_{s100} is the magnetization of bare γ-Fe_2O_3 nanoparticles (62 emu/g) at 5 kOe and room temperature.

Figure 3b shows the measured and calculated values of magnetization as a function of weight fraction of MNPs in the nanocomposite hydrogels. It can be clearly seen that the maximum magnetization values increase linearly with the increase in the magnetic nanoparticles in the hydrogels. The data points present the measured magnetization values by VSM. The solid line shows the calculated values of the magnetization according to the equation

$$\sigma_{\text{nanocomposite hydrogels}} = \text{wt \\%}_{\text{MNPs}} \times \sigma_{\text{MNPs}} \quad (2)$$

Here, wt $\%_{MNPs}$ and σ_{MNPs} are the weight fraction and saturation magnetization values of the bare magnetic nanoparticles, respectively. It can be observed that the difference in the maximum magnetization values of the nanocomposite hydrogel is only a result of decreasing of the magnetic nanoparticle content in the samples. Therefore, the free radical polymerization has not resulted in any degradation in the spontaneous magnetization of the magnetic particles, and the decrease in saturation magnetization is directly related to the weight fraction of the magnetic nanoparticles.

dx.doi.org/10.1021/es4005152 | Environ. Sci. Technol. 2013, 47, 6297−6305

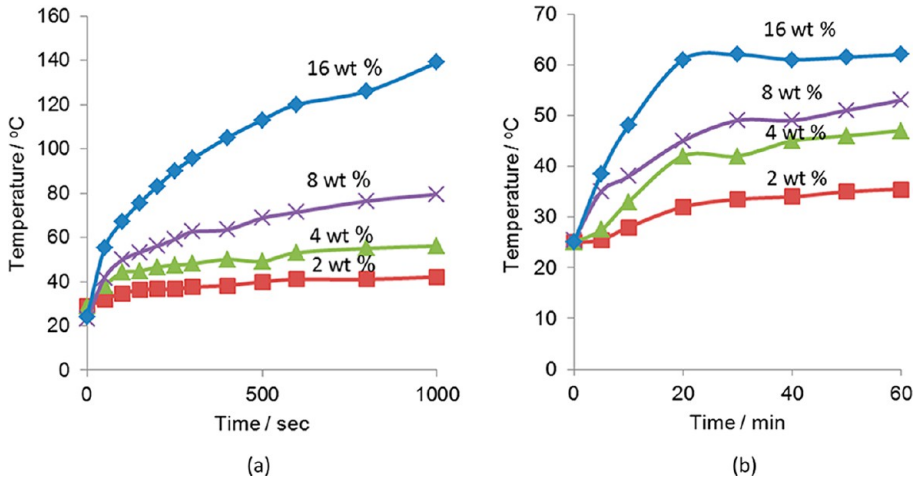

Figure 4. Temperature increase of 0.2 g of (a) dry and (b) swollen ($Q = 5$) nanocomposite hydrogels in a magnetic AC field (400.5 A, 148 Oe and 372 kHz).

For particles in a ferrimagnetic state, heating effects can be achieved in an alternating (AC) magnetic field as a result of core losses. The core loss mechanisms associated with the technical magnetization (i.e., the magnetic polarization process induced by changes of magnetic domain configurations) are mainly (i) the static hysteresis loss and (ii) the eddy current loss. The power loss by the former mechanism is simply proportional to the frequency, whereas the contribution from the latter effect increases progressively with an increase in the driving frequency because of the large phase shift between the applied field and the magnetic induction at higher frequencies. The power loss induced by the technical magnetization in the nanoparticles dissipates as heat, and thus, the heat generation rate can be controlled not only by the applied field strength but also by the frequency. Figure 4 shows the effect of an AC magnetic field on the temperature increase of 0.2 g of dry and swollen ($Q \sim 5$) nanocomposite hydrogels with different concentrations of magnetic nanoparticles. As can be seen, the temperature rises at a higher rate when the concentration of magnetic nanoparticles increases. It can also be seen that the temperatures of dry hydrogels increase much faster than that of swollen hydrogels. This is because the generated heat in the swollen hydrogels is being consumed by water to move out of the hydrogels. The specific absorption rates (SAR) were calculated (see Supporting Information Figure S5) on the basis of the calorimetric measurements and the data of the linear section of the temperature rise curves (Figure 4b). As expected, increasing the concentration of the magnetic nanoparticles resulted in an increase in the SAR values.

The effect of incorporation of MNPs into polymer hydrogels on the swelling ratio of hydrogels was studied for a period of 200 h. As can be seen in Figure 5a, the swelling behaviors of all samples are similar, as expected. The swelling process of a hydrogel particle is a function of its structural (cross-linking density and polymer network thickness and relaxation rate) and chemical (degree of solubility and ionic strength) characteristics. As shown in Supporting Information Figure S4, an increase in the concentration of MNPs in the hydrogel network led to a significant reduction in the cross-linking density of hydrogels, which should theoretically raise the swelling ratios of the hydrogels;[24] however, the enhancement in the swelling ratio rate was not observed in Figure 5a. The possible explanation for this is that the inclusion of MNPs into hydrogel

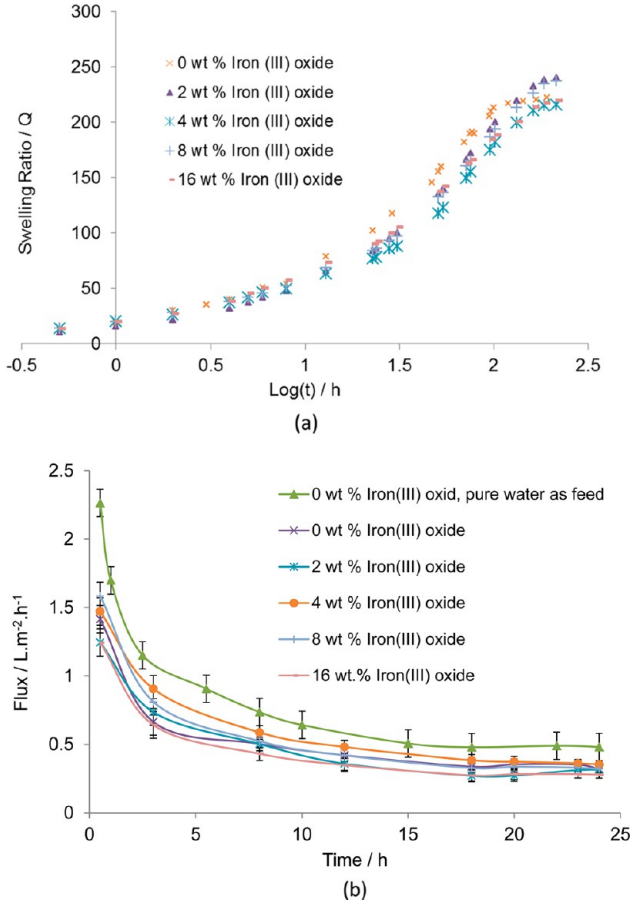

Figure 5. (a) Semilogarithmic plot of the nanocomposite hydrogels with different concentrations of Fe_2O_3 nanoparticles and (b) water flux of 0.2 g nanocomposite hydrogels with different concentrations of iron(III) oxide MNPs (pure water and 2000 ppm NaCl solution were used as feed in a 24 h FO process).

network could limit the relaxation ability, effectively acting as physical cross-links, increasing the elastic modulus (E) of the polymeric network[16,25] and thus effectively reducing the water uptake capacity and swelling ratio.[22,26] It seems that the effect of the two parameters (reduction in cross-linking density and increase in elastic modulus) on the swelling ratio largely cancel

dx.doi.org/10.1021/es4005152 | Environ. Sci. Technol. 2013, 47, 6297−6305

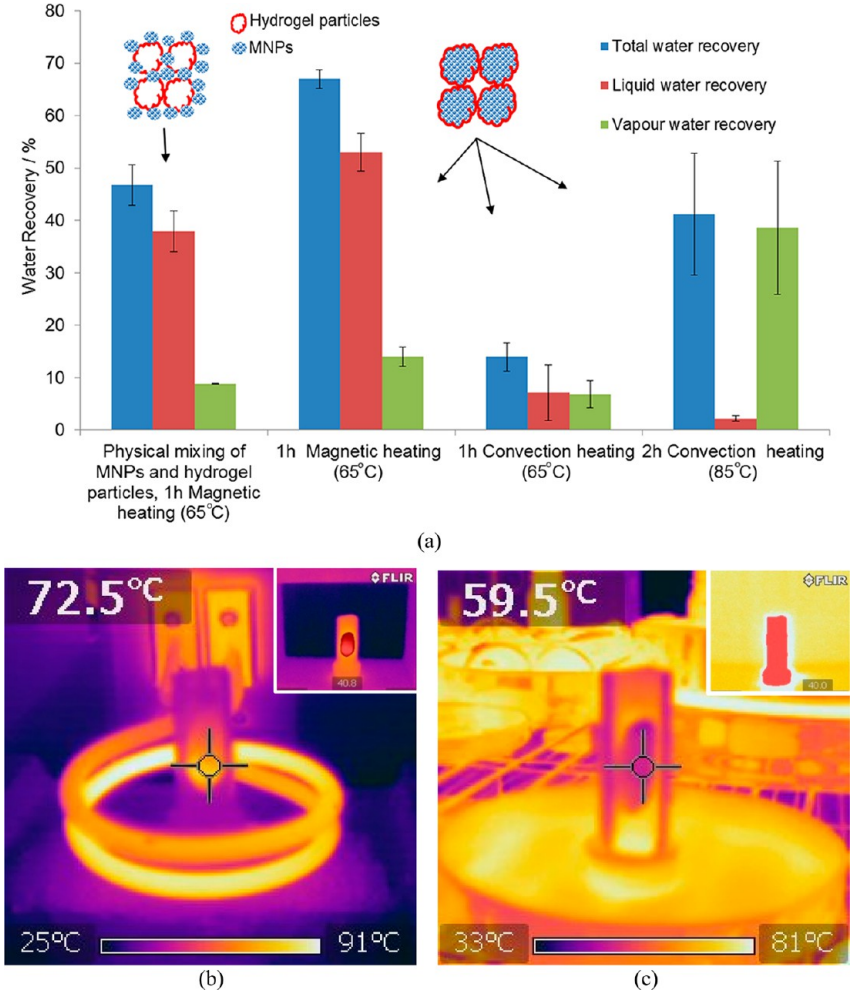

Figure 6. Water recovery of 0.2 g of nanocomposite hydrogels (swelling ratio of 6 ± 0.8) with 16 wt % MNPs (a) under magnetic field (400.5 A, 148 Oe and 372 kHz) and convection heating, (b) the cross section infrared images of 0.4 g of nanocomposite hydrogels in the dewatering cell after 25 min in the magnetic AC field (400.5 A, 148 Oe and 372 kHz), and (c) convection oven at 65 °C (the IR camera in the inset images was set to show the temperatures above 40 °C).

out each other and leave the swelling process unaffected. Since the Fe_2O_3 particles are insoluble in water and much larger than ionic species, they cannot themselves induce a higher osmotic pressure and swelling in the nanocomposite hydrogels. However, it has been reported that surface functionalization of particles can be used to generate high osmotic pressures,[27,28] and this represents another advantage of the inclusion of such particles, which is outside the scope of the work presented here.

From Figure 5a, the swelling of the hydrogel nanocomposite increase and then reach a plateau equilibrium, the magnitude of that plateau not changing much with different concentrations of MNPs. During the swelling process, water molecules diffuse into the polymer, and the polymer chains start to relax. This diffusion and relaxation process results in the formation of a swollen (rubbery polymer) region on the outer surface of the hydrogel particle and a nonswollen (glassy) inner core of the hydrogel. The diffusion rate decreases from the outer shell to the inner part of the hydrogel. The swelling ratios versus time shown in Figure 5a appear to be sigmoidal curves, which consist of an initial activation and mobility induced in the outer surfaces of the particles and, hence, an acceleration in the swelling kinetics of this region. At the early stage of the swelling process, the internal rigid core limits the swelling to only the normal direction of the outer swollen shell. The swelling process proceeds until it reaches the point where the advancing swollen front meets the rigid internal core. At this point, which corresponds to the second part of the curves, the acceleration of the swelling kinetics occurs, and the nanocomposite hydrogel particle begins to swell in all directions.[29] To predict the diffusion mechanism of the swelling process of nanocomposite hydrogels, the initial swelling data ($M_t/M_\infty \leq 0.6$) were fitted to the exponential heuristic equation.[30,31]

$$\frac{M_t}{M_\infty} = kt^n \tag{3}$$

where M_∞ and M_t are the amount of absorbed water at equilibrium hydration level and time t, respectively; n is the characteristic exponent of the transport mode; and k is the characteristic constant of hydrogel. The results revealed that the average characteristic exponent of the transport mode n for nanocomposite hydrogels is 0.496 ± 0.036, which suggests that the Fickian diffusion is most likely the diffusion mechanism. According to Alfrey et al.,[32] Fickian diffusion occurs when the diffusion rate of swelling agent (such as water) is significantly lower than the relaxation rate of polymer chains.

Figure 5b presents the water fluxes in a 24 h FO process using nanocomposite hydrogels with different concentrations of

dx.doi.org/10.1021/es4005152 | Environ. Sci. Technol. 2013, 47, 6297−6305

MNPs. For all samples, a relatively sharp decline was observed over the first 5 h, which is attributed to the driving force (osmotic pressure) reduction. Comparison between the water fluxes of pure hydrogel particles (0 wt % iron(III) oxide MNPs) with different salinities of feed solution (0 and 2000 ppm) showed that the fluxes were higher when the feed was pure water because of the greater driving force. However, the inclusion of MNPs into hydrogel network did not substantially influence the flux of the nanocomposite hydrogels.

To investigate the effect of external (convectional) and internal (magnetic) heating on the water recovery, the 0.2 g nanocomposite hydrogels with 16 wt % MNPs were placed in a convection oven at 65 and 85 °C for 1 and 2 h (see Figure 6a). As presented in Figure 6a, the water recoveries of nanocomposite hydrogels that were placed in the 65 °C convection oven for 1 h were significantly lower than those of the nanocomposite hydrogels placed in the magnetic AC field over a similar temperature range. It was also observed that raising the convection oven temperature to 85 °C and also increasing the heating period to 2 h not only did not result in a higher total water recovery compared with magnetic heating, but also reduced the liquid water recovery. A likely reason for this could be attributed to a phenomenon which is known as *case hardening* in dehydration.[33,34] During dewatering by convection heating in an atmosphere of low water activity, the nanocomposite hydrogel surface moisture content decreases abruptly to such a level that it forms a glassy rigid skin. This rigid outer shell can considerably limit further macroscopic contraction and liquid water release.[34] However, internal heat generation via magnetic heating increases the hydrogel temperature more uniformly, with an insignificant temperature gradient, thereby reducing the impact of case hardening on the dewatering rate.

To study the extent of case hardening on the water recovery, 0.032 g of Fe_2O_3 and 0.168 of g hydrogel particles were physically mixed to make 0.2 g of 16 wt % MNP−hydrogel powder (see schematics in Figure 6a). As shown, the water recoveries of the mixture in the magnetic field (1 h and 65 °C) were less than that of the nanocomposite. The total, liquid, and vapor water recoveries of the mixture were 30, 28.5, and 37% lower, respectively, than those of nanocomposite hydrogels under similar conditions. However, the water recoveries of such a mixture were significantly higher than those of nanocomposite hydrogels, which were placed in a convection oven. Therefore, the case hardening phenomenon is not the only factor that affects the water recovery rate.

Another possible contributory factor might be the temperature of the atmosphere above the sample. During the magnetic heating, the temperature of the sample increases internally in a short period of time while the surrounding atmosphere temperature increases slightly because the thermal conductivity of air/gases is an order of magnitude lower than those of polymers[35] (see Figure 6b). As the experiment proceeds, some of the water molecules locate from the sample surface to the surrounding atmosphere in the dewatering cell, which has a lower temperature than the sample. The vapor pressure increases until it approaches the point of vapor−liquid equilibrium, where the rate of evaporation is equivalent to the rate of condensation and thereby the net (overall) vapor−liquid interconversion becomes zero. This near-vapor−liquid equilibrium state of the surrounding atmosphere means that further energy generated in the MNPs due to the oscillating magnetic field is adsorbed by the remaining water molecules to move out of the hydrogel mostly in the liquid phase.

In the case of convection heating, such as in an oven, the sample temperature is lower than its surrounding dry atmosphere because the temperature of surrounding atmosphere initially increases, followed by that of the sample (see Figure 6c), which prevents the vapor and liquid phases from approaching equilibrium, and thus, evaporation proceeds. When the convection oven temperature is increased to 85 °C, a significantly higher water vapor recovery occurs because the surronding atmosphere becomes drier and has a greater capacity to hold water, and there is also a consequent increase in the evaporation rate. This is likely also the explanation for observing the higher water recoveries for samples with incorporated MNPs and stimulated internally by the oscillating magnetic field, compared with those placed in the convection oven.

Figure 7a shows the results of 1 h water recovery tests for 0.2 g of nanocomposite hydrogels with a swelling ratio of 6 ± 0.8 in the magnetic AC field (148 Oe and 372 kHz). As can be seen, the temperature and water recovery increased proportionally with the concentration of MNPs such that the total water recovery (R_t) was raised from less than 10% for a 2 wt % concentration of MNPs to around 66% for a 16 wt % concentration of MNPs. Since there is a linear relation between water recovery and MNP concentration, 100% total water recovery could be expected to be achieved at a MNP concentration of 23.7 wt %; however, serious agglomeration and precipitation of particles was observed during the hydrogel polymerization process for MNP concentrations above 16 wt %. It also can be seen from Figure 7a that desirably, the degree of the liquid water recovery was enhanced to a greater degree than that of vapor water recovery, with increasing MNP concentration. We also note that the amount of liquid water recovery via magnetic heating is significantly higher than that of mechanical pressing, which was observed in our previous work (where <4% liquid water was recovered under 30 bar hydraulic pressure).[11]

In Figure 7b, the effect of the total absolute mass of the nanocomposite hydrogels on the water recovery was investigated by fixing the water content absolute value and increasing the mass of 16 wt % nanocomposite hydrogel while keeping the swelling ratio the same. As can be seen, increasing the mass of the nanocomposite hydrogel resulted in an increase in the value of the total water recovery (R_t) from 33.45% for 0.1 g of nanocomposite hydrogel to 94.5% for 0.4 g of nanocomposite hydrogel. Although the vapor recovery increased proportionally with the mass of the hydrogel, the liquid water recovery (R_l) increased from 29% for 0.1 g of hydrogel to 53% for 0.2 g of hydrogel and then leveled off at about 60.33% for 0.4 g of hydrogel. This substantial reduction in the degree of liquid water recovery enhancement suggests that increasing the mass of hydrogel feed cannot necessarily increase the liquid water recovery, although the sample temperature increases proportionally with the mass of the hydrogel. The heating of 0.4 g of hydrogel could raise the sample temperature to around 101 °C, and this could thus raise the temperature of the surrounding atmosphere via conduction, also causing the vapor−liquid equilibrium to occur at a higher temperature. This causes more water molecules to enter the above atmosphere in the vapor phase, thus raising the vapor pressure closer to equilibrium.

The effect of changing the applied magnetic field [A/m] on the water recovery of 0.4 g of nanocomposite hydrogels with 16

dx.doi.org/10.1021/es4005152 | Environ. Sci. Technol. 2013, 47, 6297−6305

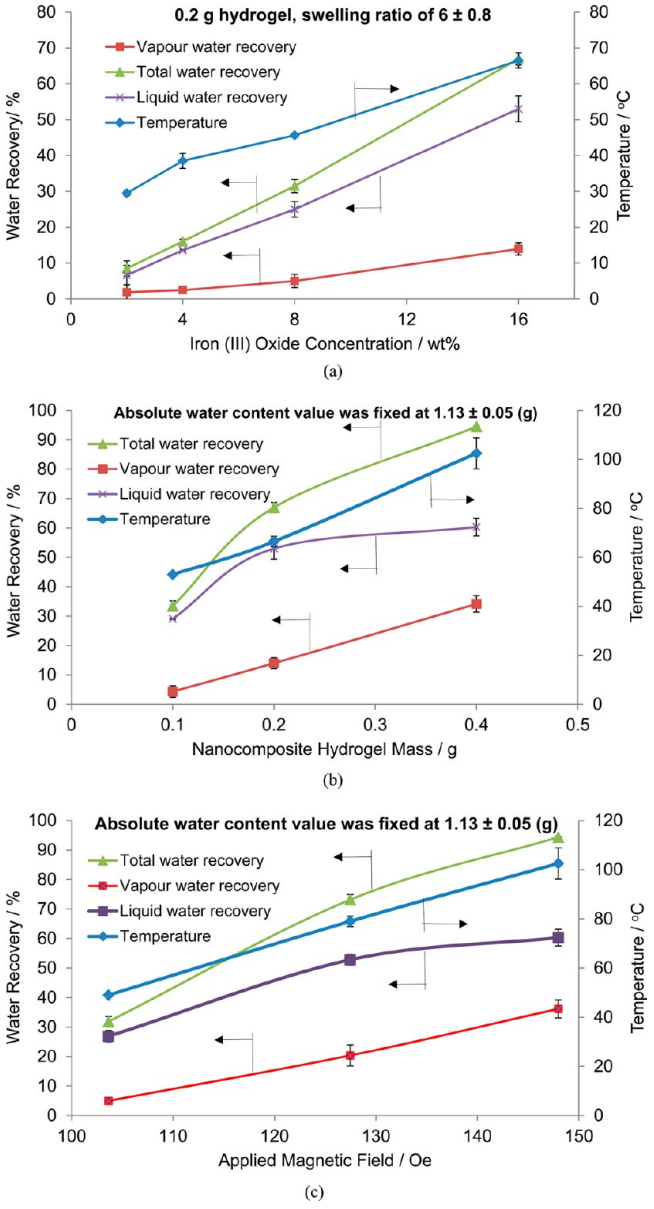

Figure 7. Effects of (a) different concentrations of MNPs, (b) different absolute mass of the 16 wt % MNP hydrogel nanocomposite and (c) different magnetic field intensities (372 kHz) on water recovery and final temperature.

wt % MNPs was investigated (Figure 7c). The applied magnetic field was calculated in oersteds,[36] as below:

$$H = \frac{ni}{\sqrt{D^2 + L^2}} \quad (4)$$

where n is the turn number of coils; i is the current; and D and L are the internal coil diameter and coil length, respectively. As can be seen, increasing the applied magnetic field intensity can proportionally increase the total water recovery. However, the liquid water recovery increased initially and then leveled off, suggesting that energy efficiency (in terms of dewatering) can be increased by reducing the applied magnetic field (Oe) and increasing the hydrogel mass.

The recyclability of nanocomposite hydrogels as a draw agent was tested in three cycles of swelling−magnetic dewatering−grinding. As can be seen in Supporting Information Figure S6, the nanocomposite hydrogels showed high recyclability without losing the performance. This suggests that the draw agent used in this work has the potential to be used in commercial and industrial applications.

The effect of incorporation of magnetic nanoparticles into the hydrogel as a draw agent on the swelling behavior, water flux, and water recovery was investigated systematically. It was also observed that liquid water recovery by means of magnetic heating for 0.2 g of 16 wt % MNPs (R_L= 53%) was significantly higher when compared with the convective heating (R_L= 7%). This could be attributed to the case-hardening phenomenon that occurs, as well as the vapor−liquid phase equilibrium of the surrounding atmosphere of the hydrogels. It was also found that increasing the absolute mass of the hydrogel sample or changing the concentration of MNPs above a certain level cannot necessarily increase the liquid water recovery, although the total water recovery can be optimized by reducing the magnetic field intensity and increasing the absolute hydrogel mass, thus leading to the maximum achievable liquid water recovery.

■ ASSOCIATED CONTENT

Ⓢ Supporting Information

Additional experimental description, XRD results (Figure S2), FT-IR spectra (Figure S3), SEM (Figure S4), SAR values (Figure S5), hydrogel recyclability (Figure S6), and magnetic properties (Table S1). This material is available free of charge via the Internet at http://pubs.acs.org.

■ AUTHOR INFORMATION

Corresponding Author

*E-mails: (G.P.S.) george.simon@monash.edu, (H.W.) E-mail: huanting.wang@monash.edu.

Notes

The authors declare no competing financial interest.

■ ACKNOWLEDGMENTS

The authors acknowledge funding from the Australian Research Council (D.P.) and also Monash Centre for Electron Microscopy (M.C.E.M.) for providing electron microscopes. H.W. thanks the Australian Research Council for a Future Fellowship.

■ REFERENCES

(1) Gil, E. S.; Hudson, S. M. Stimuli-reponsive polymers and their bioconjugates. *Prog. Polym. Sci.* **2004**, *29* (12), 1173−1222.

(2) Qiu, Y.; Park, K. Environment-sensitive hydrogels for drug delivery. *Adv. Drug Delivery Rev.* **2012**, *64* (Supplement,(0)), 49−60.

(3) Schild, H. G. Poly(*N*-isopropylacrylamide): experiment, theory and application. *Prog. Polym. Sci.* **1992**, *17* (2), 163−249.

(4) Zhang, X.-Z.; Xu, X.-D.; Cheng, S.-X.; Zhuo, R.-X. Strategies to improve the response rate of thermosensitive PNIPAAm hydrogels. *Soft Matter* **2008**, *4* (3), 385−391.

(5) Zhang, X.-Z.; Zhuo, R.-X. A novel method to prepare a fast responsive, thermosensitive poly(*N*-isopropylacrylamide) hydrogel. *Macromol. Rapid Commun.* **1999**, *20* (4), 229−231.

(6) Takata, S.-i.; Suzuki, K.; Norisuye, T.; Shibayama, M. Dependence of shrinking kinetics of poly(*N*-isopropylacrylamide) gels on preparation temperature. *Polymer* **2002**, *43* (10), 3101−3107.

(7) Serizawa, T.; Wakita, K.; Akashi, M. Rapid Deswelling of Porous Poly(*N*-isopropylacrylamide) Hydrogels Prepared by Incorporation of Silica Particles. *Macromolecules* **2001**, *35* (1), 10−12.

(8) Zhang, X.-Z.; Yang, Y.-Y.; Chung, T.-S.; Ma, K.-X. Preparation and Characterization of Fast Response Macroporous Poly(*N*-isopropylacrylamide) Hydrogels. *Langmuir* **2001**, *17* (20), 6094−6099.
(9) Gutowska, A.; Bae, Y. H.; Feijen, J.; Kim, S. W. Heparin release from thermosensitive hydrogels. *J. Controlled Release* **1992**, *22* (2), 95−104.
(10) Noguchi, Y.; Okeyoshi, K.; Yoshida, R. Design of Surfactant-Grafted Hydrogels with Fast Response to Temperature. *Macromol. Rapid Commun.* **2005**, *26* (24), 1913−1917.
(11) Li, D.; Zhang, X.; Yao, J.; Simon, G. P.; Wang, H. Stimuli-responsive polymer hydrogels as a new class of draw agent for forward osmosis desalination. *Chem. Commun.* **2011**, *47* (6), 1710−1712.
(12) Zhao, S.; Zou, L.; Tang, C. Y.; Mulcahy, D. Recent developments in forward osmosis: Opportunities and challenges. *J. Membr. Sci.* **2012**, *396* (0), 1−21.
(13) Liu, T.-Y.; Hu, S.-H.; Liu, K.-H.; Liu, D.-M.; Chen, S.-Y. Preparation and characterization of smart magnetic hydrogels and its use for drug release. *J. Magn. Magn. Mater.* **2006**, *304* (1), e397−e399.
(14) Meenach, S. A.; Hilt, J. Z.; Anderson, K. W. Poly(ethylene glycol)-based magnetic hydrogel nanocomposites for hyperthermia cancer therapy. *Acta Biomater.* **2010**, *6* (3), 1039−1046.
(15) Kumar, C. S. S. R.; Mohammad, F. Magnetic nanomaterials for hyperthermia-based therapy and controlled drug delivery. *Adv. Drug Delivery Rev.* **2011**, *63* (9), 789−808.
(16) Kato, N.; Takizawa, Y.; Takahashi, F. Magnetically Driven Chemomechanical Device with Poly(*N*-isopropylacrylamide) Hydrogel Containing γ-Fe_2O_3. *J. Intell. Mater. Syst. Struct.* **1997**, *8* (7), 588−595.
(17) Bai, H.; Liu, Z.; Sun, D. D. Highly water soluble and recovered dextran coated Fe_3O_4 magnetic nanoparticles for brackish water desalination. *Sep. Purif. Technol.* **2011**, *81* (3), 392−399.
(18) Chekli, L.; Phuntsho, S.; Shon, H. K.; Vigneswaran, S.; Kandasamy, J.; Chanan, A. A review of draw solutes in forward osmosis process and their use in modern applications. *Desalin. Water Treat.* **2012**, *43* (1−3), 167−184.
(19) Ling, M. M.; Chung, T.-S.; Lu, X. Facile synthesis of thermosensitive magnetic nanoparticles as "smart" draw solutes in forward osmosis. *Chem. Commun.* **2011**, *47* (38), 10788−10790.
(20) Li, D.; Zhang, X.; Yao, J.; Zeng, Y.; Simon, G. P.; Wang, H. Composite polymer hydrogels as draw agents in forward osmosis and solar dewatering. *Soft Matter* **2011**, *7* (21), 10048−10056.
(21) Goswami, S.; Kiran, K.; Panda, A. B.; Sharma, P. P.; Mahapatra, S. K.; Bhoraskar, S. V.; Banerjee, I. Synthesis of magnetically active interpenetrating polymer network for drug release. *Int. J. Nano Dimens.* **2011**, *2* (1), 37−48.
(22) Galicia, J. A.; Cousin, F.; Dubois, E.; Sandre, O.; Cabuil, V.; Perzynski, R. Static and dynamic structural probing of swollen polyacrylamide ferrogels. *Soft Matter* **2009**, *5* (13), 2614−2624.
(23) Mørup, S.; Hansen, M. F.; Frandsen, C. Magnetic interactions between nanoparticles. *Beilstein J. Nanotechnol.* **2010**, *1*, 182−190.
(24) Duracher, D.; Elaïssari, A.; Pichot, C. Preparation of poly(*N*-isopropylmethacrylamide) latexes kinetic studies and characterization. *J. Polym. Sci., Part A: Polym. Chem.* **1999**, *37* (12), 1823−1837.
(25) Kato, N.; Yamanobe, S.; Takahashi, F. Property of magneto-driven poly(*N*-isopropylacrylamide) gel containing γ-Fe_2O_3 in NaCl solution as a chemomechanical device. *Mater. Sci. Eng., C* **1997**, *5* (2), 141−147.
(26) Satarkar, N. S.; Hilt, J. Z. Magnetic hydrogel nanocomposites for remote controlled pulsatile drug release. *J. Controlled Release* **2008**, *130* (3), 246−251.
(27) Ge, Q.; Su, J.; Chung, T.-S.; Amy, G. Hydrophilic Superparamagnetic Nanoparticles: Synthesis, Characterization, and Performance in Forward Osmosis Processes. *Ind. Eng. Chem. Res.* **2011**, *50* (1), 382−388.
(28) Ling, M. M.; Wang, K. Y.; Chung, T.-S. Highly Water-Soluble Magnetic Nanoparticles as Novel Draw Solutes in Forward Osmosis for Water Reuse. *Ind. Eng. Chem. Res.* **2010**, *49* (12), 5869−5876.
(29) Gerlach, G., Arndt, K.-F., Eds. *Hydrogel Sensors and Actuators*; Springer: Heidelberg, New York, 2010.
(30) George, K. A.; Wentrup-Byrne, E.; Hill, D. J. T.; Whittaker, A. K. Investigation into the Diffusion of Water into HEMA-co-MOEP Hydrogels. *Biomacromolecules* **2004**, *5* (4), 1194−1199.
(31) Kayaman, N.; Okay, O.; Baysal, B. M. Swelling of polyacrylamide gels in polyacrylamide solutions. *J. Polym. Sci., Part B: Polym. Phys.* **1998**, *36* (8), 1313−1320.
(32) Alfrey, T.; Gurnee, E. F.; Lloyd, W. G. Diffusion in glassy polymers. *J. Polym. Sci., Part C: Polym. Symp.* **1966**, *12* (1), 249−261.
(33) Khalloufi, S.; Bongers, P. Mathematical investigation of the case hardening phenomenon explained by shrinkage and collapse mechanisms occurring during drying processes. *Comput.-Aided Chem. Eng.* **2012**, *30*, 1068−1072.
(34) Bar, A.; Ramon, O.; Cohen, Y.; Mizrahi, S. Shrinkage behaviour of hydrophobic hydrogel during dehydration. *J. Food Eng.* **2002**, *55* (3), 193−199.
(35) Razmjou, A.; Arifin, E.; Dong, G.; Mansouri, J.; Chen, V. Superhydrophobic modification of TiO_2 nanocomposite PVDF membranes for applications in membrane distillation. *J. Membr. Sci.* **2012**, *415−416* (0), 850−863.
(36) Cullity, B. D.; Graham, C. D. Experimental Methods. In *Introduction to Magnetic Materials*; John Wiley & Sons, Inc.: New York, 2008; pp 23−86.